Efficient and monolithic polarization conversion system based on a polarization grating

Jihwan Kim,[1] Ravi K. Komanduri,[1] Kristopher F. Lawler,[1]
D. Jason Kekas,[2] and Michael J. Escuti[1,*]

[1]Department of Electrical and Computer Engineering, North Carolina State University, Raleigh, North Carolina 27695, USA

[2]ImagineOptix Corporation, 7202 Doverton Court, Raleigh, North Carolina 27615, USA

*Corresponding author: mjescuti@ncsu.edu

We introduce a new polarization conversion system (PCS) based on a liquid-crystal polarization grating (PG) and louvered wave plate. A simple arrangement of these elements laminated between two microlens arrays results in a compact and monolithic element, with the ability to nearly completely convert unpolarized input into linearly polarized output across most of the visible bandwidth. In our first prototypes, this PG-PCS approach manifests nearly 90% conversion efficiency of unpolarized to polarized for ±11° input light divergence, leading to an energy efficient picoprojector that presents high efficacy (12 lm/W) with good color uniformity.   © 2012 Optical Society of America

OCIS codes: 120.4640, 260.5430, 050.1950, 230.3720, 230.5440, 120.2040.

1. Introduction

Although nearly all liquid-crystal (LC) displays and devices operate on polarized light, the vast majority of light sources are unpolarized, including the lamps and light-emitting diodes (LEDs) most common in data projectors and LC display backlights. Polarizers are easily employed, but they inherently work by absorbing or redirecting the unwanted polarization, leading to at most 40%–50% (unpolarized to polarized) conversion efficiency. Such large loss is obviously undesirable, especially in portable and high brightness display systems [1].

For the most part, two approaches are used to improve conversion efficiency. The first recycles the unwanted polarization by reflecting it back into the light source itself, where its polarization will be at least partially scrambled and subsequently reemitted with the desired polarization [2]. This preserves the étendue of the light source and commonly leads to around 55%–70% conversion efficiency. The second approach [3–6], called a polarization conversion system (PCS), involves only a single pass. One set of elements spatially separates the incident light into two orthogonal polarizations, typically a fly-eye lens and a polarizing beam splitter (PBS) array, and then a final element selectively converts only one of these polarizations into the other, typically a louvered half-wave plate. While conversion efficiency can be around 60%–70% [7] and the light source is homogenized, this approach doubles the étendue. Perhaps even more importantly, the efficiency substantially degrades for input divergence angles beyond ±5° [7], limited mainly by the polarization splitting element (i.e., the PBS array). This PBS array is also challenging to fabricate, and all three individual elements are challenging to align with the needed precision.

In 2005 [8], an alternative polarization splitting element was suggested: the novel diffractive element called a polarization grating (PG), composed of a holographically patterned birefringent material with periodic optical axis [9,10]. When formed with LCs [11–14], PGs act essentially as thin-film PBSs that can split unpolarized light into two orthogonal

circular polarizations with high efficiency (95%–99%) for fairly large incident angles [10] and wide bandwidths [15]. As shown in Fig. 1(a), the output diffraction angle is governed by the classic grating equation, $\sin\theta_{\pm1} = \pm\lambda/\Lambda + \sin\theta_{\mathrm{in}}$, where Λ is the grating period and $\theta_{\pm1}$ and θ_{in} are the first-order diffracted and incidence angles, respectively. As initially proposed within two primitive PCS designs [8], the PG was used to create and separate the orthogonal polarizations, followed by subsequent elements to convert one polarization into the other.

In 2011, an improved PCS was demonstrated [7], where the PG essentially replaces the PBS array in the conventional PCS, with minor variations: a PG with a laminated quarter-wave plate (QWP) on its output was arranged before the fly-eye lens, followed by the louvered half-wave plate. This PG-based PCS was designed for a $\pm7°$ light source and offered 80% peak conversion efficiency compared to 70% for an equivalent conventional PCS using the PBS array. While this demonstrated that the high efficiency and wider angular acceptance of the PG made it an effective replacement for the PBS array, the configuration was far from optimized. First, each element was separate, meaning there were six air interfaces leading to reflection losses, and each required individual precision alignment by an external fixture. Second, there were two individual retardation elements performing the polarization conversion, a job that could be done with a single element. These issues added complexity and hamstrung the polarization conversion efficiency.

2. Monolithic PG-PCS Concept

Here we describe a new PCS design that achieves nearly complete polarization conversion in a monolithic package. This approach is based on the idea of arranging both the PG and wave plate elements after a first lens, as illustrated in Fig. 1(b). Incident light is focused by the lens into two spots at the focal plane, corresponding to the first-order beams diffracted by the PG. The light in these two spots is circularly polarized, with orthogonal handedness. A patterned retarder with two zones is then arranged at the focal plane. When this retarder has broadband quarter-wave retardation everywhere, but different optical axes (e.g., $\pm45°$) in each zone, it will convert the two orthogonal circular polarizations into the same linear polarization. The PG period Λ is chosen such that collimated light at the center wavelength λ (e.g., 550 nm) is diffracted to the center of these two zones. This geometry defines the diffraction angle $\theta_{\pm1} = \tan^{-1}(D/4f)$, where D is the lens diameter and f is the focal length. Then Λ is calculated using the classic grating equation:

$$\Lambda = \frac{\lambda}{\sin(\tan^{-1}(D/4f))}. \tag{1}$$

The monolithic PG-PCS concept is an expansion of this, illustrated in Fig. 1(c). A functional PCS for projectors must be compact, and the output angles usually need recollimation. We therefore place a microlens array (MLA) at both the input and output. These MLAs are usually two-dimensional arrays, but may also be one dimensional. Each lenslet behaves approximately the same as the discrete lens described in Fig. 1(b), resulting in two orthogonally polarized grids of spots at the focal plane, interspersed but spatially separated. Both Λ and f must be chosen to optimize the polarization conversion, constrained by the divergence of the incident light and the limitations on lenslet dimensions (i.e., achievable lens curvature, lateral size, and substrate thickness). Equation (1) is a good rule of thumb. Another is that approximately complete polarization conversion only occurs when the input divergence angle $\pm\theta_{\mathrm{DIV}}$ is $\leq\theta_{\pm1} = \sin^{-1}(\lambda/\Lambda)$, since there is no overlap of each focal plane spot onto its neighboring patterned retarder. However, even when $\pm\theta_{\mathrm{DIV}} > \theta_{\pm1}$, the degradation is often minimal. As these rules of thumb neglect many details, optical ray-trace modeling tools are needed to determine optimum designs.

The patterned retarder, known as a louvered wave plate (LWP), must now have two zones per lenslet, but only in the single dimension corresponding to the PG diffraction plane. As before, these zones should have the same achromatic quarter-wave retardation,
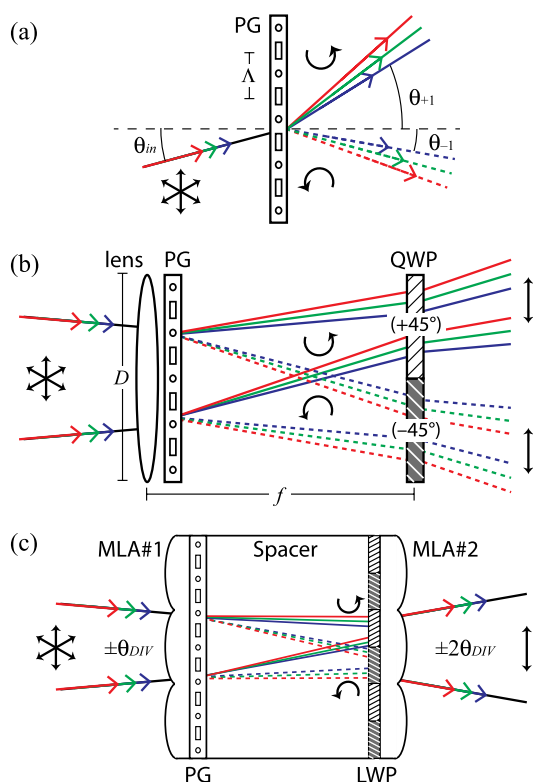

Fig. 1. (Color online) (a) PG behavior and geometry; (b) macroscopic concept of polarization conversion from unpolarized to linearly polarized using a lens, PG, and two quarter-wave plates (QWPs); and (c) our monolithic PG-PCS concept, with two microlens arrays (MLAs). $\pm\theta_{\mathrm{DIV}}$ is the divergence angle of the light.

but with orthogonal optical axes. With the LWP arranged near the focal plane, both grids of orthogonal circular spots are converted into the same linear polarization. Finally, the second MLA is positioned close to the LWP at the focal plane and registered with the first MLA in order to both homogenize and recollimate the output before being relayed by additional optics onto the microdisplay.

One obvious feature is that all elements may be laminated together because the only nonplanar surfaces are facing outward. This monolithic design leads to lower loss due to interface reflections and simplifies the alignment of the PCS into an optical system. The conversion efficiency is not only enhanced, but the overall fabrication cost and integration complexity is reduced.

3. Component Fabrication and PCS Assembly

We fabricated PGs and LWPs using commercial materials and processing and formed custom MLAs using standard methods. For both the PG and LWP, we used the material LIA-C001 (DIC Corp.) for the photoalignment polymer and reactive LC prepolymer mixture RMS10-025 ($\Delta n \sim 0.16$, EMD Chemicals, Inc.) doped with chiral LCs CB-15 and MLC-6247 (also EMD Chemicals, Inc.) as detailed below. Both elements were formed on 1 mm thick borosilicate glass substrates, using spin coating. All elements were laminated together using the optical adhesive NOA-65 (Norland).

We formed the PG with a 3.6 μm period, leading to a diffraction angle of $\pm 8.5°$ at 530 nm, using UV-laser polarization holography and methods described in [15]. The total first-order diffraction efficiency ($\eta_{+1} + \eta_{-1}$) for unpolarized input was measured for various input divergence angles. As shown in Fig. 2, the PG shows high (>95%) diffraction efficiency within substantial divergence input angles ($\pm 11°$). This wider angular aperture of PGs is a principle reason
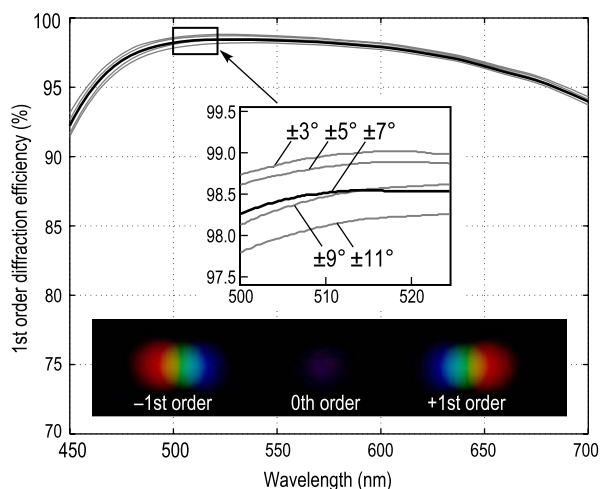
PGs have higher throughput in a PCS than a PBS array [7].

The LWP contains alternating zones that behave like broadband QWPs with $\pm 45°$ optical axis orientations and was fabricated using the methods described in [16]. First, the photoalignment material is exposed to a UV lamp through a chrome mask with alternating transparent and opaque zones with 0.7 mm width, which is mounted on a translation stage. This is a two-step process where a linear polarizer is used to adjust the exposure directions to 0° and 90° when the corresponding zones are exposed. This patterned alignment layer was then coated with two LC polymer layers on top of each other to build up a broadband QWP known as a multi-twist-retarder [16]. The first layer had a twist angle of $-90°$ and a thickness of 1.36 μm, while the second layer had a twist angle of $+60°$ and a thickness of 0.83 μm. We characterized the quarter-wave by sending circularly polarized input into a single zone and measuring the fraction of light output with the correct linear (e.g., S) and incorrect (e.g., P) polarization. A representative spectrum of this is shown in Fig. 3 and was substantially the same for both zones. The output is predominantly linearly polarized (i.e., >97% correct, and <3% incorrect) over the entire visible range. Similar measurements were obtained using a commercial measurement tool (Axoscan).

The two identical MLAs were formed by injection molding of an acrylic molding resin (Plexiglas) into a 5-by-9 grid of lenslets, each with 1.4 mm × 0.77 mm dimension and 1.1 mm spherical radius of curvature. A single-layer antireflection (AR) coating was applied on the lenslet outer surface. A glass spacer of 1 mm thickness was used to distance the LWP at the focal plane of the first MLA.

The PG, LWP, and glass spacer were fabricated on 1 in. square substrates and subsequently diced

Fig. 2. (Color online) PG characterization: first-order diffraction efficiency ($\eta_{+1} + \eta_{-1}$) spectrum of a PG with a 3.6 μm grating period for various input light divergence in visible range; (inset) a photograph of unpolarized, white LED light diffracted by a PG.
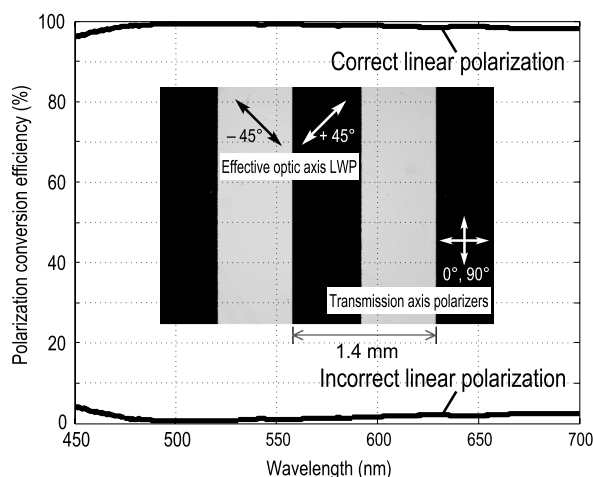

Fig. 3. LWP characterization: polarization conversion efficiency of an LWP converting circular polarization into linear polarization; (inset) picture of the LWP placed between crossed polarizers. A second nonlouvered QWP was inserted between the LWP and polarizer to show the contrast between the two LWP zones.

to match the size of the MLAs. These were then glued together by hand with the use of a polarizing optical microscope to register the MLAs and the LWP. The resulting monolithic PG-PCS [Fig. 1(c)] was ~4 mm thick.

4. PG-PCS Performance

In order to characterize PCS polarization conversion, we used the optical setup illustrated in the inset of Fig. 4(a). A broadband unpolarized white light source with controllable divergence angle (3° to 11°) was used for characterization. The output was analyzed by a linear polarizer in a rotation mount and collected into an integrating sphere connected to a fiber spectrometer (Ocean Optics, Inc.). The absorption of the polarizer itself was normalized out so that the polarization conversion efficiency is essentially defined as the transmittance of the PCS with a perfect analyzing polarizer; therefore, a perfect PCS manifests 100%, and an empty measurement (no PCS at all) would show 50%.

The experimental PG-PCS indeed showed very good polarization conversion. As shown in Fig. 4(a) for ±7° divergence angle, the output contained 90% correct linear polarization (correct here implies the desired PCS output polarization, e.g., vertical linear) for most of the visible range (520–650 nm), and low (<4%) incorrect polarization (incorrect here refers to the polarization orthogonal to the desired PCS output, i.e., horizontal linear). The incorrect polarization normally needs to be removed with a clean-up polarizing optic, such as a PBS cube, or a sheet polarizer. This 90% peak is directly comparable to the 80% of the prior PCS with PGs [7] and substantially higher than any conventional PCS with a PBS array.

A photo of the PG-PCS itself and the output beam is shown in Fig. 4(b). The output beam had ±7° × ±14° divergence, confirming the expected doubling of étendue. We also note qualitatively that the brightness and color uniformity of the output is outstanding, just like the prior PCS based on PGs [7].

Several factors negatively affect performance. First, the baseline transmittance of the MLAs alone was only 95% (i.e., a null PCS containing only the glass spacer and no PG or LWP), due to reflection, absorption, haze, and deflection into larger angles. Second, the PG and LWP manifest nonideal behavior for obliquely incident light (>15°): the PG diffraction efficiency is reduced as light leaks into the zero-order directions remaining unpolarized, and the LWP retardation deviates from quarter-wave. Third, the MLA acrylic material itself manifests some measurable but minor birefringence, which can cause the output polarization to degrade. Fourth, misalignment in relative position and orientation of the elements can cause loss; the distance between the first MLA and the LWP is perhaps most critical. Finally, at larger divergence angles, the first-order spots at the LWP begin to overlap with their neighbors, which further reduces conversion efficiency even though
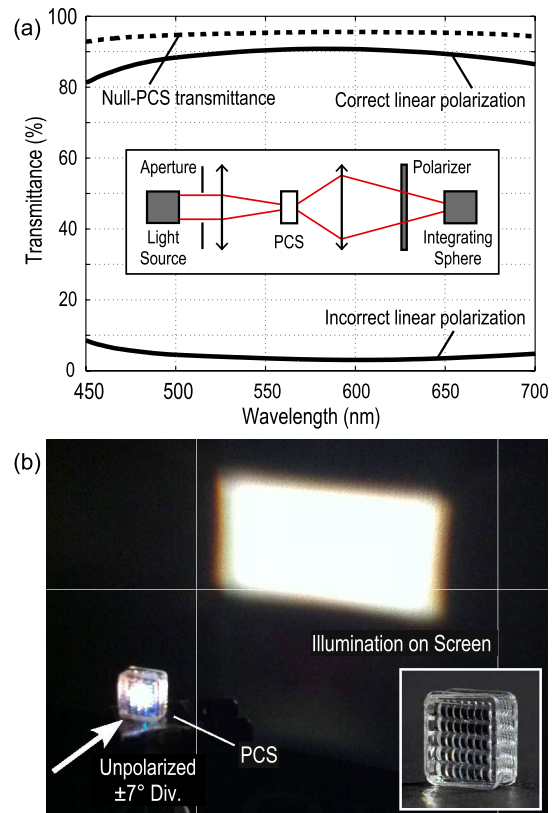

Fig. 4. (Color online) (a) Measured PCS performance showing ≈90% correct polarization transmittance in most of the visible range, (inset) layout of the PCS characterization setup. (b) Illumination of the PCS on a screen, (inset) a photograph of the PCS.

the diffraction efficiency of the PGs may still be high. We anticipate that improvements in the AR coatings of the MLAs and retardation compensation of the LWP would be particularly effective to improve the conversion efficiency and effective acceptance angle even further.

We also measured the PCS performance for various θ_{DIV} to explore the dependence on angular aperture. The fraction of correct polarization is shown in Fig. 5. For small input divergence (±3°, ±5°), the PCS output is almost completely polarized correctly (92%), approaching the null-PCS curve (95%). This indicates that the individual elements are well aligned, and the difference between the two may be explained by some combination of the LWP incorrect polarization conversion (Fig. 3) and a small zero-order leakage of the PG (Fig. 2). For larger divergence angles, a slow degradation occurs likely due to the larger oblique incidence on the PG and LWP. However, note the polarization conversion is high (80%–87%) even at ±11°.

5. PG-PCS Projector Prototype

To demonstrate the effectiveness of the PG-PCS within a display system, we custom built a prototype picoprojector. As shown in Fig. 6(a), the optical design is conventional in its basic approach: light from three LEDs (OSRAM) was combined with dichroic
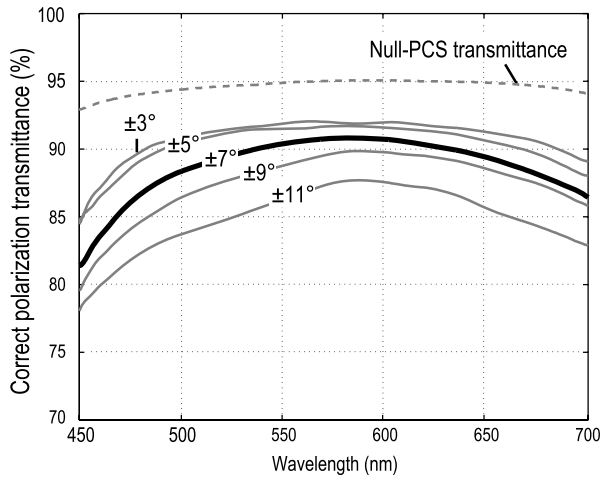
Fig. 5. PCS transmittance of the correct polarization for various input divergence angles.

mirrors, relayed into a PBS cube (Foreal Spectrum, Inc.), and directed onto a WVGA (854×480) LC-on-silicon (LCoS) microdisplay (Syndiant, Inc.). A PG-PCS was positioned immediately before the PBS cube, with only slightly different parameters than those already described (i.e., shorter MLA focal length and smaller PG period).

Most importantly, the picoprojector showed a high efficacy of 12 lm/W. It manifest 10 lm brightness at 0.83 W, along with 200:1 contrast ratio (full-on-full-off), at 60 Hz full color frame rate. The "box" volume of the entire projector [Fig. 6(b)] was 6.2 cm^3, with a thickness of 6.8 mm.

Several photographs of images produced by this picoprojector are shown in Fig. 7. The brightness uniformity of the projected images ($\sim$36 in. diagonal) is outstanding. The grid of 3×3 numbers in the top left image are relative luminance values at those positions within the image; it shows a uniformity ratio of 86% ($=$ min/max luminance) for white and all colors individually and standard deviation of 0.064.

For comparison, we examined a commercial picoprojector (i.e., inside Sony Camcorder HDR-PJ260 V). The following data resulted, from measurements conducted in the same way as above: 9 ± 1 lm/W efficacy, 11 lm brightness, 250:1 contrast, nHD (640×360) resolution. Most notably, its uniformity ratio was 57% and standard deviation 0.29, producing an image dramatically less uniform to an observer. Our picoprojector also compares favorably to the only prior PG-based PCS projector [7], which manifests 9 lm/W efficacy, 9 lm brightness, and $\sim$70% uniformity within 10 cm^3.

To isolate the effect of the PG-PCS itself, we replaced it with a null PCS and found the brightness dropped to 6.1 lm, showing that the PG-PCS enhanced the brightness by a factor of 1.64. This
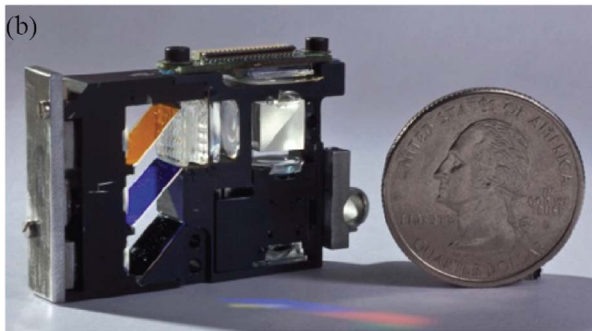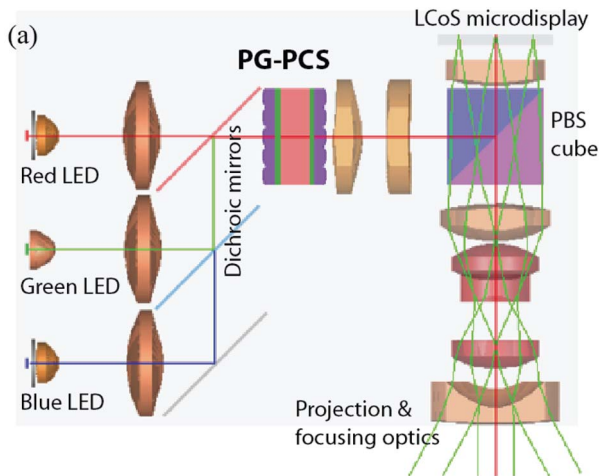

Fig. 6. (Color online) (a) Optical layout of the prototype picoprojector based on PG-PCS. (b) Photograph of the picoprojector.

Fig. 7. (Color online) Photographs of images projected by the prototype picoprojector using the PG-PCS.

suggests that the PG-PCS in this particular projector performed with 82% polarization conversion, including the photopic weighting, similar to the radiometric curves in Fig. 5.

In summary, the PG-PCS enabled our picoprojector prototype to perform extremely well, producing a more uniform image in a smaller volume and with substantially higher efficacy than all accessible comparisons. It is important to note that a PG-PCS can be used with similar benefit within larger LC projectors and adapted into back/front lights for any display using polarized light.

6. Conclusion

We have described a PCS that converts unpolarized to linearly polarized light with high efficiency. It is based on a broadband PG that angularly separates incident light into orthogonal circular polarizations, while an LWP converts each to the same linear polarization, both arranged in between two MLAs. We demonstrate >90% peak conversion efficiency at ±7°, and 80%–87% at ±11°. Avenues to improvement beyond this are straightforward. The PG-PCS is a compact and easily aligned monolithic element, unlike prior approaches. We also built a picoprojector around this element, with 12 lm/W luminous efficacy, 10 lm brightness, class-leading image uniformity, and 6.2 cm^3 volume, which demonstrates the high efficiency benefits of the PG-PCS.

References

1. M. S. Brennesholtz and E. H. Stupp, *Projection Displays* (Wiley, 2008).
2. M. F. Weber, O. Benson, Jr., S. Cobb, Jr., J. M. Jonza, A. J. Ouderkirk, D. L. Wortman, and C. A. Stover, "Display with reflective polarizer and randomizing cavity," U.S. patent 6,025,897 (15 February 2000).
3. Y. Itoh and T. Hashizume, "Polarization conversion element, polarization illuminator, display using the same illuminator, and projection type display," U.S. patent 5,986,809 (16 November 1999).
4. D. F. Vanderwerf, "Polarized illumination system for LCD projector," U.S. patent 5,995,284 (30 November 1999).
5. M. Duelli and A. T. Taylor, "Novel polarization conversion and integration system for projection displays," SID Int. Symp. Dig. Tech. Pap. **34**, 766–769 (2003).
6. J. K. Slack, M. V. Khazova, T. Takatsuka, K. Mitani, K. Inoko, G. J. Woodgate, M. Hara, G. Bourhill, and E. Walton, "Polarization separation element, a polarization conversion system, an optical element, and a projection display system," U.S. patent 6,621,533 (16 September 2003).
7. E. Seo, H. C. Kee, Y. Kim, S. Jeong, H. Choi, S. Lee, J. Kim, R. K. Komanduri, and M. J. Escuti, "Polarization conversion system using a polymer polarization grating," SID Int. Symp. Dig. Tech. Pap. **42**, 540–543 (2011).
8. M. J. Escuti, C. Sanchez, C. W. M. Bastiaansen, and D. J. Broer, "Polarization gratings in mesogenic films," U.S. patent 8,064,035 (22 November 2011).
9. L. Nikolova and T. Todorov, "Diffraction efficiency and selectivity of polarization holographic recording," Opt. Acta **31**, 579–588 (1984).
10. C. Oh and M. J. Escuti, "Numerical analysis of polarization gratings using the finite-difference time-domain method," Phys. Rev. A **76**, 043815 (2007).
11. G. P. Crawford, J. N. Eakin, M. D. Radcliffe, A. Callan-Jones, and R. A. Pelcovits, "Liquid-crystal diffraction gratings using polarization holography alignment techniques," J. Appl. Phys. **98**, 123102 (2005).
12. M. J. Escuti, C. Oh, C. Sanchez, C. Bastiaansen, and D. J. Broer, "Simplified spectropolarimetry using reactive mesogen polarization gratings," Proc. SPIE **6302**, 630207 (2006).
13. S. R. Nersisyan, N. V. Tabiryan, D. M. Steeves, and B. R. Kimball, "Optical axis gratings in liquid crystals and their use for polarization insensitive optical switching," J. Nonlinear Opt. Phys. Mater. **18**, 1–47 (2009).
14. R. K. Komanduri and M. J. Escuti, "High efficiency reflective liquid crystal polarization gratings," Appl. Phys. Lett. **95**, 091106 (2009).
15. C. Oh and M. J. Escuti, "Achromatic diffraction from polarization gratings with high efficiency," Opt. Lett. **33**, 2287–2289 (2008).
16. R. K. Komanduri, J. Kim, K. F. Lawler, and M. J. Escuti, "Multi-twist retarders for broadband polarization transformation," Proc. SPIE **8279**, 82790E (2012).